



City Research Online

## City, University of London Institutional Repository

---

**Citation:** Guerrato, D., Nouri, J. M., Stosic, N., Arcoumanis, C. & Smith, I. K. (2008). Flow measurements in the discharge port of a screw compressor. *Proceedings of the Institution of Mechanical Engineers, Part E: Journal of Process Mechanical Engineering*, 222(4), pp. 201-210. doi: 10.1243/09544089jpme200

This is the accepted version of the paper.

This version of the publication may differ from the final published version.

---

**Permanent repository link:** <https://openaccess.city.ac.uk/id/eprint/14334/>

**Link to published version:** <https://doi.org/10.1243/09544089jpme200>

**Copyright:** City Research Online aims to make research outputs of City, University of London available to a wider audience. Copyright and Moral Rights remain with the author(s) and/or copyright holders. URLs from City Research Online may be freely distributed and linked to.

**Reuse:** Copies of full items can be used for personal research or study, educational, or not-for-profit purposes without prior permission or charge. Provided that the authors, title and full bibliographic details are credited, a hyperlink and/or URL is given for the original metadata page and the content is not changed in any way.

---

City Research Online:

<http://openaccess.city.ac.uk/>

[publications@city.ac.uk](mailto:publications@city.ac.uk)

---

# Flow measurements around the discharge port of a twin screw compressor

## FLOW DEVELOPMENT IN THE DISCHARGE CHAMBER OF A SCREW COMPRESSOR

Diego Guerrato, Jamshid M. Nouri, Nikola Stosic, C Arcoumanis and Ian K Smith  
School of Engineering and Mathematical Sciences  
City University, London EC1V OHB, U.K.

### ABSTRACT

The angle-resolved mean and turbulence characteristics of axial air flow within the rotors and discharge chambers of a screw compressor have been measured, using a laser Doppler velocimeter (LDV) with high spatial and temporal resolution. The measurements were made through special transparent windows fixed in the compressor casing and in the exhaust pipe immediately above the discharge port. Results were obtained at a speed of 1000 rpm, a discharge pressure 1 bar and a temperature of 57°C.

The flow interaction between the rotors and the discharge chamber was established as well as the spatial variation of the axial mean velocity and turbulence velocity fluctuation. It was shown that the discharge flow was complex, strongly time dependent and controlled by several mechanisms. In general, the axial velocity, on entering the working chamber, downstream of the discharge port exit was higher than that immediately upstream with large variation in mean and RMS velocities immediately after the opening of the discharge port, then flow becomes more uniform. The high velocity values and large fluctuation are mainly controlled by the pressure gradient across the port at the very beginning of the discharge process, after that, as the port opens wider, uniform flow is influenced mainly by the rotor action.

These measurements will be used as input data, for more reliable optimisation of compressor design, and also to validate a CFD model of fluid flow within twin screw compressors, already developed in-house.

**Keywords:** Screw Compressor, Laser Doppler Velocimetry, Cycle-resolved averaging

### NOTATION

$D_p$ main rotor pitch diameter	$V_p$ Pitch axial velocity
$H_p$ axial position of the CV (rotor chamber)	$Y_p X_p Z_p$ cartesian coordinate of the CV (discharge)
$R_p$ radial position in the CV (rotor chamber)	$\alpha_p$ angular position of CV (rotor chamber)
$Re$ Reynolds number	$\phi$ helix angle at the pitch diameter
$n$ compressor speed	$\mu$ viscosity

$\rho$  density

## INTRODUCTION

The operating principle of screw machines, as expander or compressors, has been known over 120 years. Despite this, serious efforts to produce them were not made until low cost manufacturing methods became available for accurate machining of the rotor profiles. Since then, great improvements have been made in performance prediction, rotor profile design and manufacturing techniques. Screw compressors are now highly efficient, compact, simple and reliable. Consequently, they have largely replaced reciprocating machines for their majority of industrial applications and in many refrigeration systems. Screw compressor and expanders are positive displacement machines. They consist essentially of a pair of meshing helical rotors, which rotate within a fixed casing that encloses them and provide access to the suction and discharge conducts without the necessity of valves as within reciprocating machines. The compression process occurs inside several volumes called working chambers that bring gas from the suction squeeze and then deliver it within the outlet port. Figure 1 put in evidence in which way one of the working chamber goes through the all process as the rotors move.



**Figure 1:** Screw compressor working principle

Although screw machines can work as expander or compressors, their overwhelmingly common use is as compressors. Mainly there are two types, oil flooded, commonly known as oil injected, and oil free compressors. Figure 2 shows two examples of them for similar rotor sizes.

In oil injected compressors, air and oil are mixed up together within the machine and then separated in a special equipment installed downstream the compressor. At this stage air is released to the high pressure line and oil is being cooled and injected into the compressor again. The oil acts as a lubricant between moving parts, a sealant of any clearances between the rotors and between the rotors and the casing and as a coolant of the gas during the compression process. That cooling effect is the key factor which allows pressure ratios of approximately 15:1 in a single stage without get an excessive temperature at the discharge side. Typical oil-gas mass ratio 4:1 or even more.

Now days screw compressor components can be manufactured with tolerances of order of  $\pm 5$  micron and internal clearances are usually 30-60 micron.

In oil free compressors, only gas is admitted into the working chamber and internal shaft seals, located between the bearings and compression chamber at each end of the rotor, are needed. Seals prevent oil, which is supplied to the bearings through an external lubrication system, from entering the working chamber and thereby contaminating the gas being processed. In such dried conditions, a contact between rotors is strongly inadvisable and usually synchronization is obtained by external gears.

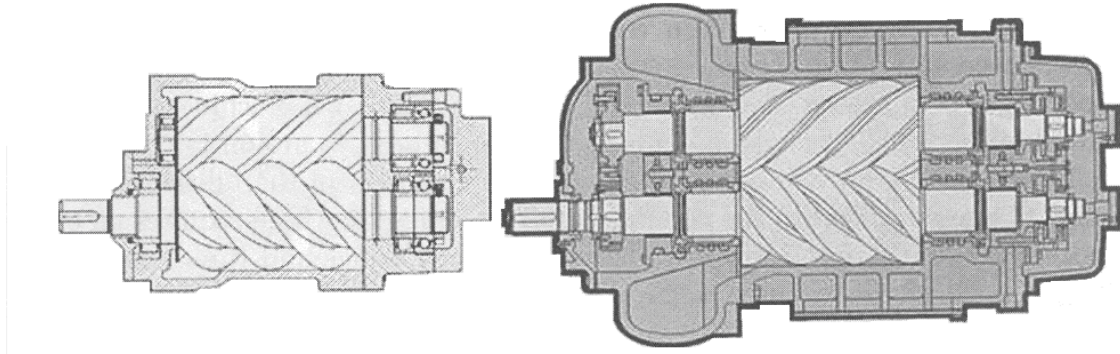


**Figure 2:** flooded and dry screw compressor types

Since there is not oil injection, gas is being compressed at a final temperature much higher than in oil flooded compressors for similar working conditions. As a consequence of that pressure ratios are limited to approximately 3:1, depending on the type of gas being compressed.

Working temperature of the order of magnitude of 250 °C, creates thermal expansion and affects the relatively small clearances in the rotor meshing region and between rotors and casing, therefore to avoid unsafe contacts, clearances have to be much larger than in a flooded compressor. Since there is not sealing supplied by oil and flow passages are larger, gas losses among a working chambers are higher and reduce machine performances.

It is believed that the adiabatic efficiency of oil free compressors could be increased by as much as 10% if minimum safe clearances could be predicted accurately.

The advanced method of predicting screw compressors performances are well known and has already been described in some detail in [2&5]. However, to make further improvements and optimise the design, it is essential to have a good understanding of the gas flow by quantifying the velocity field in the suction, discharge and working chambers and, especially, through the clearance gaps based on a 3-D model, so as to characterize the whole sequence of processes that occur within the compressor.

The total number of papers published on the flow characteristics within twin-screw compressors is rather small compared to the published work on other types of machine such as a turbocharger. Many overall measurements of screw compressor performance have been reported, such as those in [2&5]. However, the investigations of [1, 3 & 4] seem to be the only reported experimental works on flow behaviour in screw compressors or screw superchargers in which local quantitative measurements are described.

The material presented in this paper is part of a long term research project attempting to measure the fluid mean velocity distribution and the corresponding turbulence fluctuations at various cross-sections across the discharge chamber to characterise the flow development through the port of the compressor at different phase angles. The overall aim is to reveal how major features of the fluid flow within the machine are affected by the rotor geometry and operating conditions.

In addition to the flow measurements, other properties of the compressor, such as the suction and discharge pressures and temperatures have been measured with standard laboratory-type instruments and compared with predicted values of the same properties derived from an existing CFD model [5]. This comparison has allowed validation and further development of the CFD package to a stage which will render it possible to design future screw compressors without the need for expensive and time-consuming experiments.

As described above, the flow in screw compressors is complex, three-dimensional and strongly time-dependent similar to the in-cylinder flows in gasoline and diesel engines [6-7], centrifugal pumps [8], or in turbocharger turbines [9-11] and mixing reactors [12]. This implies that the measuring instrumentation must be robust to withstand the unsteady aerodynamic forces, have high spatial and temporal resolution and, most important, must not disturb the flow. Only point optical diagnostics like LDV can fulfil these requirements, as demonstrated by previous research in similar flows. The preferred method of research is to characterise the fluid mean velocity and turbulence fluctuations at a range of pre-selected measurement points using a dual beam Laser-Doppler Velocimeter (LDV).

The same dual beam LDV system as that described in [1&3] was used to obtain the angle-resolved axial mean and the turbulence characteristics of the flow inside the rotor and discharge chamber of a standard air compressor. Measurements were performed on both the male and female rotors in the interlobe region and inside the discharge cavity at several positions. This was made possible through transparent windows made of plexiglass (Perspex), which provided optical access for the laser beams and backscatter signal acquisition.

## **FLOW CONFIGURATION AND INSTRUMENTATION**

The transparent windows for optical access into the rotor chamber of the test compressor were machined from acrylic to the exact internal profile as the rotor casing, and were positioned at the pressure side of the compressor near the discharge port, as shown in figure 3. After machining, the internal and external surfaces of the window were fully polished to allow optical access. The optical access to the discharge chamber was through a transparent plate, 20 mm thick, installed on the upper part of the exhaust pipe. The optical compressor was then installed in the standard laboratory air compressor test rig, modified to accommodate the transmitting and collecting optics and their traverses, as shown in figure 6.

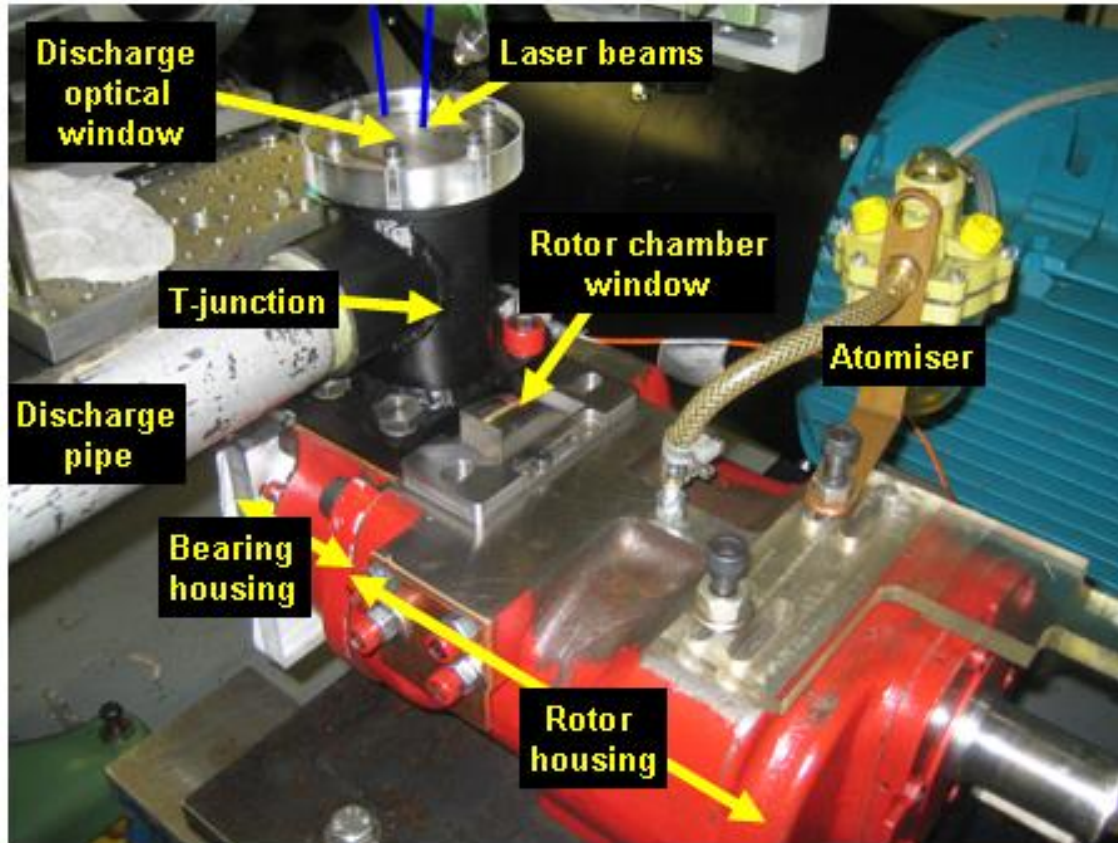


**Figure 3** : Optical compressor equipped with transparent windows near the discharge;

Figures 4 (a), (b) and (c) show the discharge chamber (divided into discharge port and discharge cavity), the measurement locations, the coordinate system and a schematic description of the flow motion within the entire working chamber. From the images it is clearly evident that the port cross-section on the rotor side is very different from that on the cavity side and this greatly influences the flow transformation through it. The resulting flow is very complex and will be analysed in more detail later. The discharge port cross-section area in contact with the rotors chamber is shaped like a reversed double delta as shown in figures 4(b),(d) and will be referred to as the W-section. This cross-section is contracted and reduced considerably on the cavity side of the port to form a single inverted delta shape, which will be referred to as the V-section. Those shapes are shown in figures 4(c), (d) and (e). The coordinate system drawn in all the sketches identifies the CV location. Measurements were made at  $X_p=5.5\text{mm}$ ,  $Z_p=13\text{mm}$  and  $Y_p=-8$  to  $13\text{mm}$ .

Two more coordinate systems were defined within the rotor chamber of the compressor. Figures 5 (a), (b) and (c) show the coordinate systems applied for each rotor where  $\alpha_p$  and  $R_p$  are, respectively, the angular and radial position of the control volume and  $H_p$  is the distance from the discharge port centre. Taking the appropriate coordinate system, measurements were obtained at  $R_p=48, 56, 63.2\text{mm}$ ,  $\alpha_p=27^\circ$  and  $H_p=20\text{mm}$  for male rotor, and at  $R_p=42, 46, 50\text{mm}$ ,  $\alpha_p=27^\circ$  and  $H_p=20$  for female rotor. In addition, due to different inner surface curvatures of casing with male and female rotors, two different windows were machined for optical access as can be seen in figure 5(a) and (b).

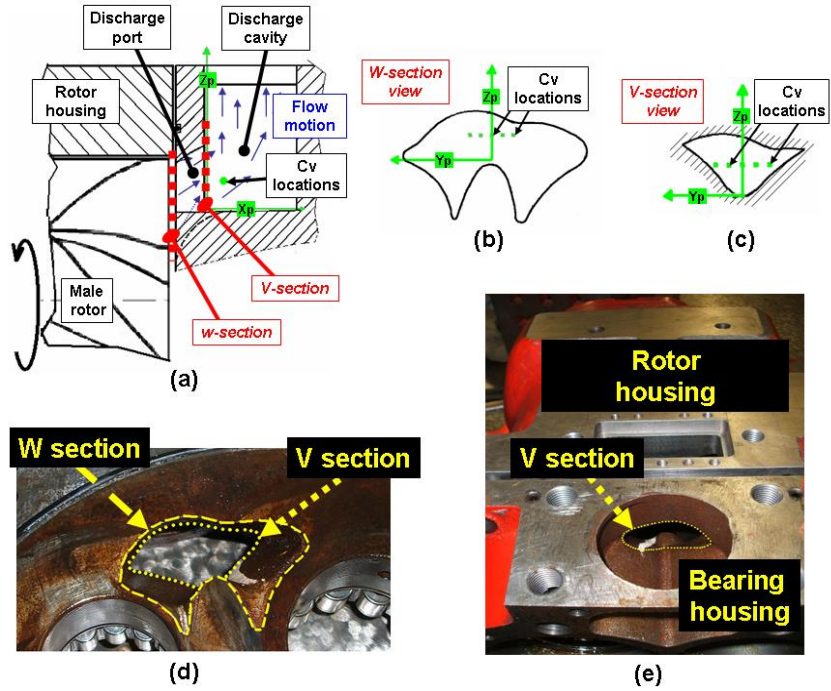


**Figure 4:** Geometry of the compressor at the outlet port: (a) Transverse-section of the discharge (b) W section view, (c) V section view; (d) Actual discharge port viewed from rotors side; (e) Actual discharge port viewed from cavity side

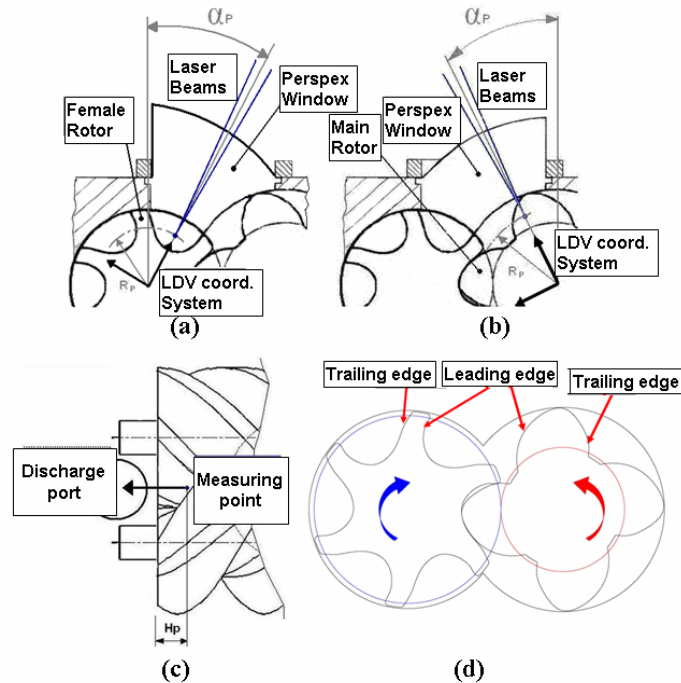


**Figure 5:**(a) Coordinate system and window adopted for female rotor; (b) Coordinate system and window adopted for male rotor; (c) Axial plane view; (d) view, of male and female rotor edges.

Figure 6 shows the main components of the laser Doppler Velocimeter which was operating in the dual-beam near backscatter mode. It comprised a 700 mW argon-Ion laser, a diffraction-grating unit to divide the light beam into two and provide frequency shift and collimating and focusing lenses to form the control volume. A fibre optic was used to direct the laser beam from the laser to the transmitting optics, and a mirror was used to direct the beams from transmitting optics into the compressor through one of the transparent windows. The collecting optics were positioned around  $25^\circ$  for the rotor chamber and  $15^\circ$  for the discharge chamber to the full backscatter position and comprised collimating and focusing lenses, a  $100\ \mu\text{m}$  pin hole and a photomultiplier equipped with an amplifier. Despite the crossing region of the laser beams is an ellipsoid more than 0.5 mm long, the size of the pinhole defines the effective length of the measuring volume so that it can be represented as a cylinder 100 high with  $79\ \mu\text{m}$  diameter. The fringe spacing is  $4.33\ \mu\text{m}$ . The signal from the photomultiplier was processed by a TSI processor interfaced to a PC and led to angle-averaged values of the mean and RMS velocities. In order to synchronise the velocity measurements with respect to the location of the rotors a shaft encoder that provides one pulse per revolution and 3600 train pulses, an angular resolution of  $0.1^\circ$  was used and fixed at the end of the driving shaft. Instantaneous velocity measurements were made over thousands of shaft rotations to provide a sufficient number of samples; in the present study the average sample density was 1350 data per shaft degree. Since the TSI software is provided by 4 external channels, one of them was used to collect the pressure signal coming from the high data rate pressure transducer via an amplifier.

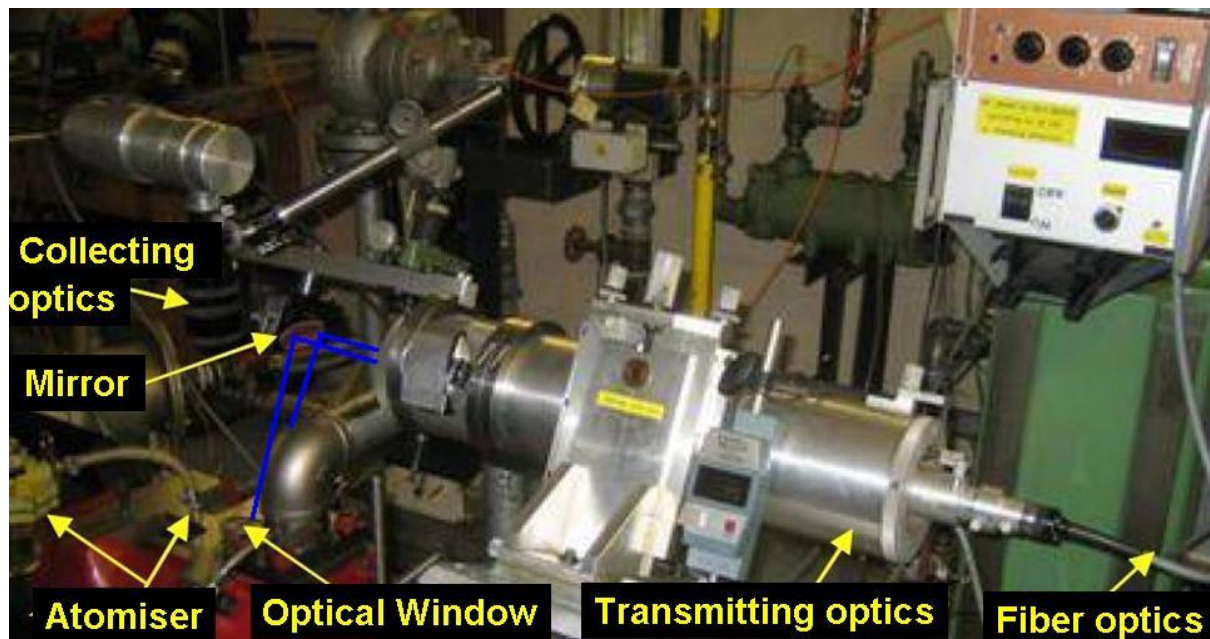


**Figure 6:** LDV optical set up of transmitting and collecting optics.

The pressure samples were collected together with the incoming velocity and matched with the instantaneous position of the shaft. The flow was seeded by a silicone oil atomiser that produces droplet sizes in the range of 1 to  $2\ \mu\text{m}$ . A low viscosity silicone oil

of 5 cSt was used. The pre-processed data produced by LDV system appear as in figure 7 (a) and were collected continuously as the compressor works in a time interval of up to 25 minutes. Although, the flow is turbulent and there is not a unique velocity value for a certain angle, some information about flow structure can be obtained. That is possible applying the so-called ‘gated post processing method’. This method consist in subdividing the data domain into many vertical areas, like the one presented in figure 7(a) with straight line and green dots, and applying statistical analysis. Then, mean and RMS values can be calculated and plotted in graphs like the ones on figures 9, 10 and 11. As already described on [1&3] this method proved to be efficient only if the angular resolution is well chosen according with data distribution and velocity gradient. For discharge port measurements, the best angular resolution was found to be  $1.0^\circ$  and, apart from a few critical points, it gave a minimum of 600 samples per analysed area, corresponding to statistical uncertainties of less than 1.7% and 5.5% for the ensemble mean and RMS velocities, based on a 95% confidence level and velocity fluctuations of the order of 20% of the mean value.

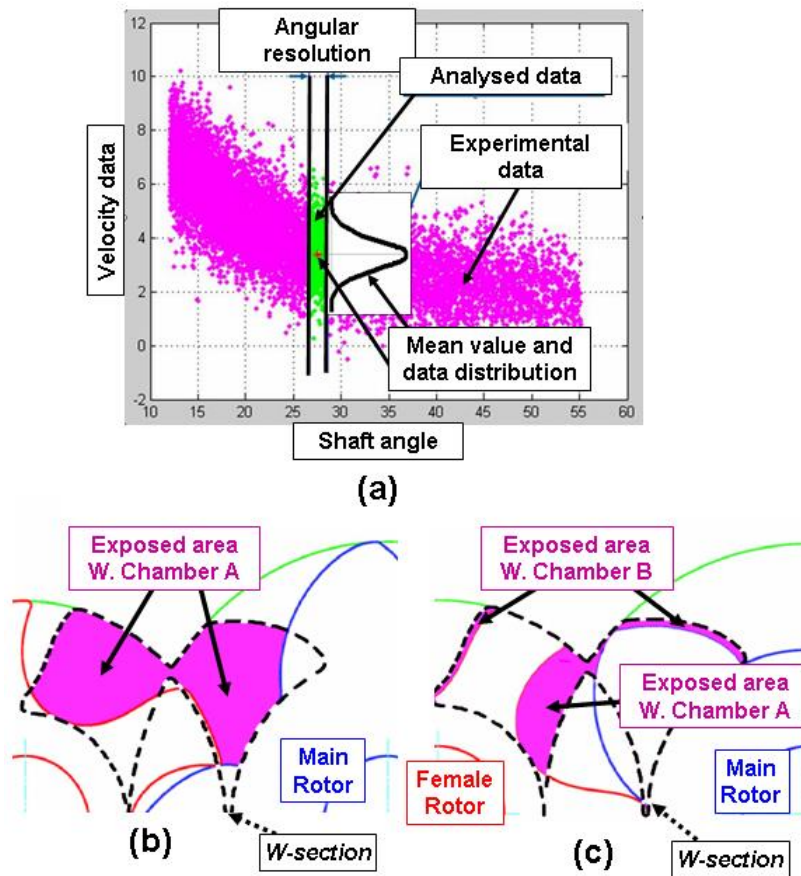


**Figure 7:** (a) Gated post processing method. (b) Exposed area for a single working chamber. (c) Combined exposed areas for two separate working chambers.

As explained in [3], it wasn't possible to obtain the desired LDV measurements under oil flooded conditions. Thus, in order to be able to measure the velocity field, the compressor was operated on air with no oil injection. Measurements were made at a speed of 1000 rpm and a discharge temperature of  $57 \pm 3^\circ\text{C}$ . The flow regime was identified by the Reynolds number estimation  $Re = \rho V_p D_p / \mu$ , where  $V_p = (2\pi n / 60)(D_p / 2) \tan(\varphi)$ . Assuming  $D_p = 81.8\text{mm}$ ,  $\varphi = 42.73^\circ$  and  $n = 1000\text{ rpm}$ ,  $V_p$  was found to be  $3.940\text{m/s}$ ; while the calculated Reynolds number was 17700. Therefore the flows at this speed can be considered turbulent. The volumetric flow rate through the compressor was measured by an orifice plate installed in the exhaust pipe and was found to be  $1.047\text{ m}^3/\text{min}$ .

## RESULTS AND DISCUSSION

The discharge process of the working fluid from the rotor chambers to the exhaust line takes place through the port and cavity of the discharge chamber of the compressor. As mentioned above, figure 4 show different plane views of this part and its two distinct "W" and "V" cross-section profiles. To clarify the flow process through the discharge port, measurements were made at the inlet (upstream of the W-section) and outlet (downstream of the V-section) and are presented below, together, to characterise the flow transformation or development through the discharge chamber.

To understand the flow motion taking place through the discharge port of the machine, some geometrical features have to be taken in consideration:

- Firstly, the W-section area, which is in contact with the rotors and connecting the rotor chamber to the discharge port, is not, the one through which the mass exchange happens. This region named exposed-area, changes at every angular position of the rotors and is smaller than physical port inlet area. It is shown schematically in figure 7(b) and (c). It is worth noting that the exchange area varies considerably according to the rotor position. Moreover, as the discharge process takes place over an angular displacement wider than the angle corresponding to a single working chamber, two contiguous discharge processes overlap. figure 7(c) shows clearly that, in fact, while fluid is discharging from a generic working chamber (A) a new process is just starting for the next called working chamber (B).
- Secondly, observing the geometrical features of the discharge port, it is possible to figure out that the air leaving the rotor chambers has to converge towards the centre and the top of the discharge port before entering into the discharge cavity and then the exhaust pipe. During this path, the air flow has to pass through several sections, especially the V-section which is the narrowest of the discharge chamber. Thus, the flow velocity is very high there and consequently turbulence rises and part of the flow energy is dissipated into heat.

The analysis of the flow downstream the V-section can provide useful information to understand how the discharge process develops and consequently on how to minimize the losses inside the compressor. With this purpose, several measuring points near the V-section were selected as shown by the row of spots in the middle of the window in figure 4(a),(b) and (c). The Cartesian reference system employed is also represented in the same figures with its origin positioned on the plane and in the lowest point of the V-section.

The points have been chosen at the shortest distance ( $X_p=5.5$ ) from the surfaces of the rotors chamber to assure suitable measuring conditions: a good Signal to noise ratio, (SNR) and the absence of strong reflections as was observed with the measurements inside the rotor chambers [3].  $Z_p=13$  mm is the elevation position in which the highest velocities are expected because it is close to the centre of the V-section.

The main mechanisms that influence the flow development through the discharge port are the difference between the internal and discharge pressures at the W-Section as soon as the discharge port opens, the rotor movement that pushes the air towards the discharge chamber, the variation of the exposed-area through which the fluid flows at the discharge port, and finally the formation of pressure waves that pass through the fluid. These four mechanisms can act simultaneously during the discharge process, however, for different conditions; some of them are more significant than others.

To describe carefully the discharge process within the compressor it is necessary to evaluate both the flow behaviour upstream and downstream the discharge port. Assuming that the air is moving mainly axially from one chamber to the next one, here only the axial velocity component was considered. A detailed description of flow behaviour within interlobe region was already provided in [1], but before presenting the current results it is important to remember the influence of the discharge port opening on the axial flow. Figure 8 illustrates schematically the trend of axial velocity profiles at certain radial locations and exhibits three different zones:

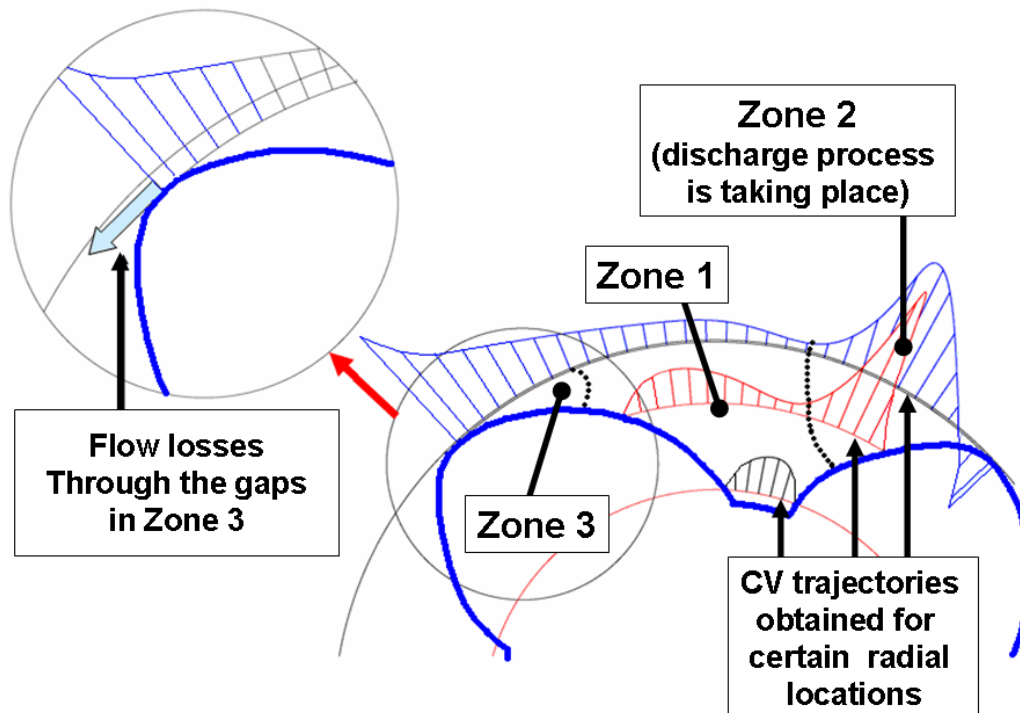


**Figure 8:** Schematic representation of flow structure within the interlobe region.

- Zone (1) where the velocity decreases towards a defined value around the middle of the working chamber .

- Zone (2) in which all velocities exhibit a sudden high and consistent acceleration that reached its peak and then decelerates. This trend was the same for all measured locations. A similar pattern was observed for turbulence which is relatively very high compared with that of zone 1. Here, the flow is influenced mainly by the pressure difference between the rotor and the discharge chamber and also by the opening area at the discharge port, rather than by other parameters such as the working chamber motion.
- Zone (3) This is influenced mainly by the leakages through the gaps between the rotors and the casing.

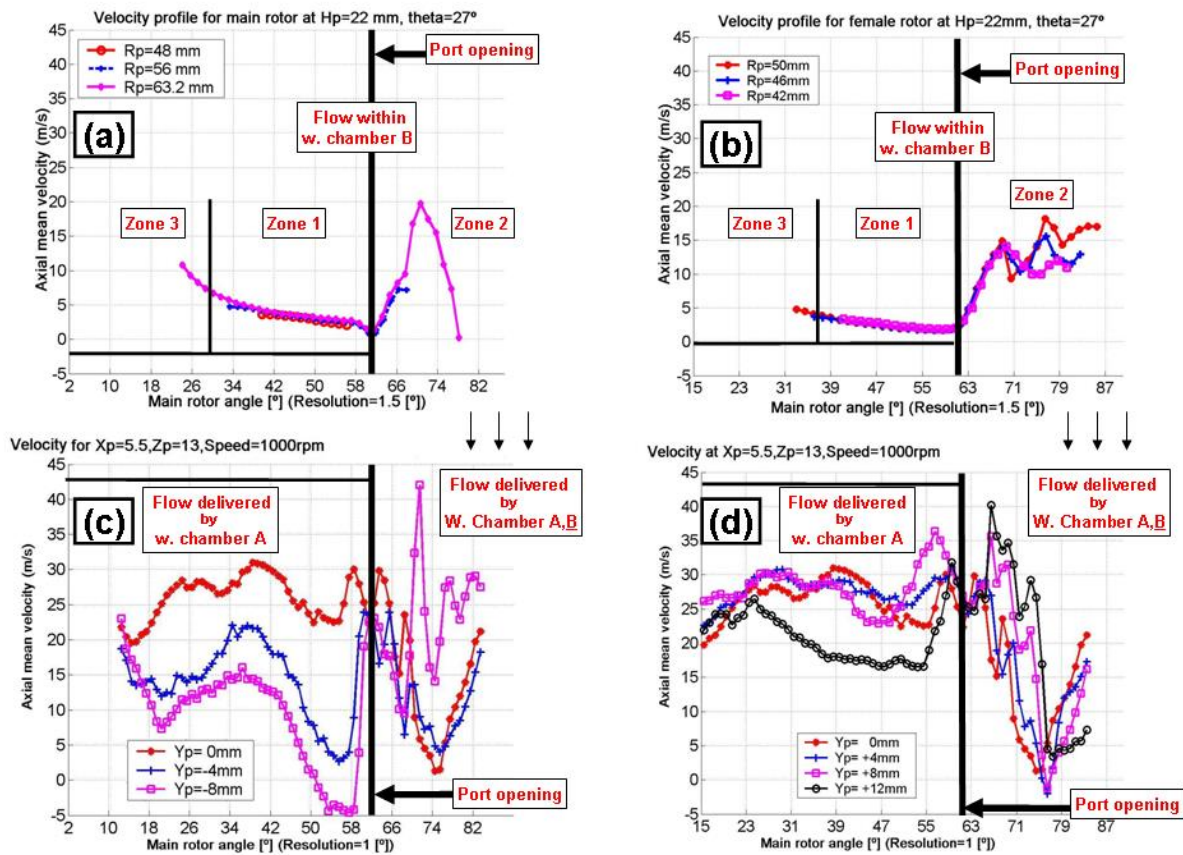


**Figure 9** Comparison between discharge axial mean velocity component at the inlet (rotor side) and outlet (cavity side) of the discharge port: (a) Inlet main rotor curves (b) Inlet female rotor curves; (c) Outlet curves of the port region close to the main rotor (d) Outlet curves of the port region close to the female rotor.

In the present measurements, the control volume was positioned within the interlobe region at an axial plane of  $H_p=20\text{mm}$  for both male and female rotors which was the closest plane to the W-section that could have been reached with the present optical setup. At the outlet of the discharge port, the nearest axial plane was 5.5mm to the V-section. The results of axial velocity at the inlet and outlet of the discharge port are

presented and compared in figure 9. The results presented in figure 9(a) and (b) refer to male and female rotors, respectively, upstream the W-section, while figure 9(c) and (d) refer to the discharge port close to the V-section. To be able to understand and explain the flow behaviour at the discharge port outlet, it is important to know how the flows from the male and female rotor's chambers are exposed and interacts into the discharge zone. This is demonstrated schematically in figure 7(b) and shows the flow from working chambers (A) of both rotors are mixed and exposed into the discharge; the display in figure 7(b) depicts a relative position of both rotors which give the maximum flow exposure into the discharge. As the rotors turn the exposed area (A) reduces until a point where the flow from the next working chambers (B) are being exposed into the discharge zone, figure 7(c). This indicates the flow exposure from one working chamber to the next is continually changing causing a complex discharge flow which would be time dependent, three dimensional, unsteady and highly turbulent.

Considering the flow feathers describe above and looking at the graphs of figure 9 then it is easy to understand that Zone 2 is the most important flow feature that will influence the flow development in the discharge port cavity as shown in figures 9(c) and (d) for the same angular position of zone 2, on the male and female sides, respectively. The bold black lines drawn on the graphs are to identify the exact angular position of the port opening.

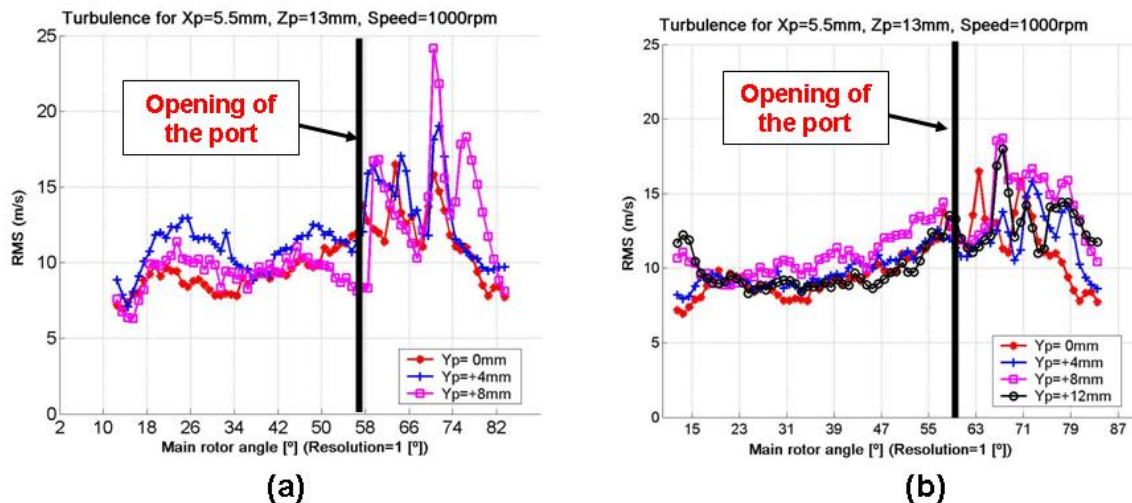


**Figure 10** Axial RMS velocity variation on the outlet of the discharge port: (a) Outlet curves of the port region close to the main rotor (b) Outlet curves of the port region close to the female rotor.

What are clearly evident observing values obtained at the discharge volume on figure 9 is the considerably higher velocities with respect to those found in the rotor regions. This big difference can be explain looking at the rather small size of the V-section compared with W-section at the inlet forming a contracting flow passage which causes fluid acceleration. In addition, once the compressed high pressure air at the end of the rotors is exposed to the low pressure discharge chamber, the flow momentum will increase and become very changeable. This trend is evident on all the curves. The flow structure was

discovered to be very complex and at least three distinct peaks are recognisable. Also, there is a tendency for the peaks to shift to higher velocities as soon as the control volumes move away from the centre of V-section towards its edges on both sides. On the left hand side of diagrams, before the opening line, the flow motion is smoother with higher variations on the main rotor side. Figures 10(a) and (b) represent the axial RMS velocity variation at the outlet of the discharge port and correspond to those of figure 9(c) and (d). In general the RMS profiles follow those of the mean velocity with large fluctuations immediately after the opening of the port.

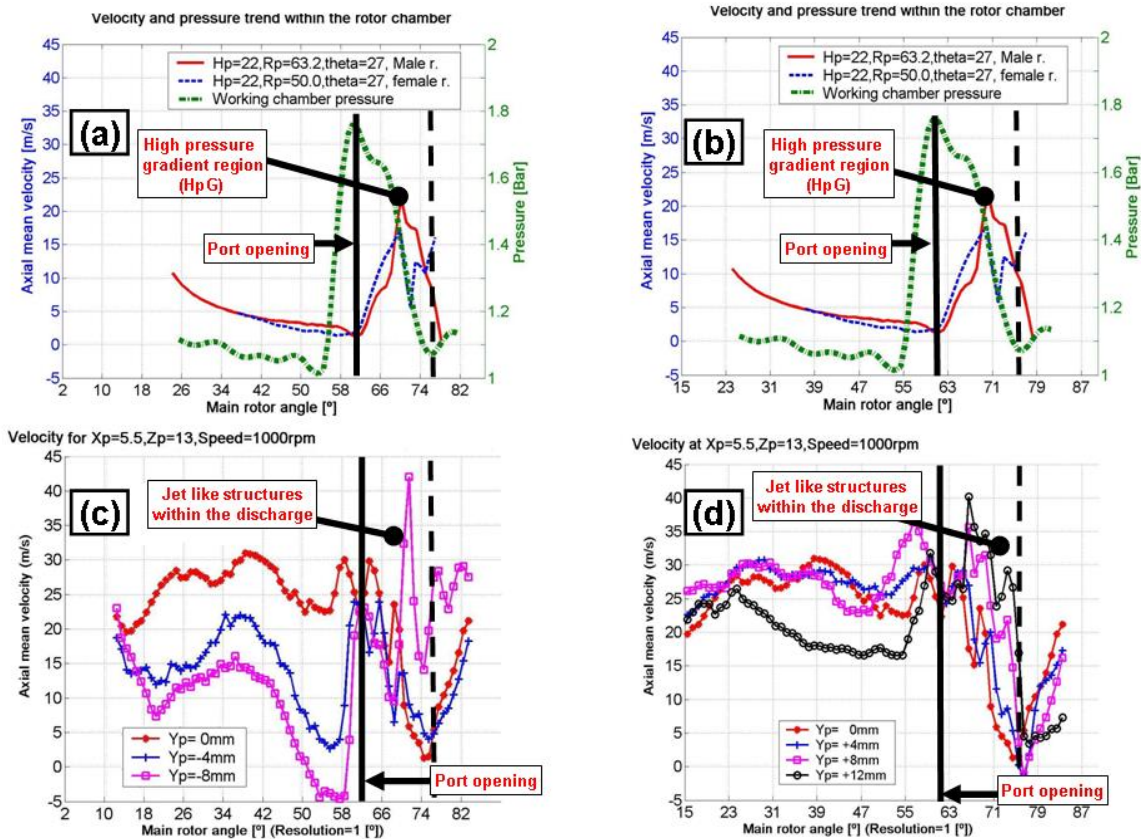


**Figure 11** Effects of pressure difference on velocity fields: (a) Main rotor curves (b); Female rotor curves; (c) Outlet curves of the port region close to the main rotor, (d) Outlet curves of the port region close to the female rotor.

To explain better the observed changes in the mean flow, the absolute pressure and the mean velocities are presented together in figure 11 at the axial location of  $H_p=20\text{mm}$ . The thick dashed curves, shown in figure 11(a) and (b), provides the absolute pressure difference within rotors and discharge chamber. Following those curves, it is possible to introduce two new important areas one on the male rotor side and another on the female side. Those areas are characterised with high pressure gradient and therefore are called the high pressure gradient regions (HpG). The elevated pressure gradient at the W-section causes strong axial mean velocity gradients, peaks and large turbulence variation. On the rest of the diagrams, where the pressure difference between the chambers is quite small, air flow is smoother and turbulence lower. This happen because pressure is quite uniform

and flow is simply due to the rotors that, like a piston, push the air out of the chamber through the V-section area.

Flow structure displayed in HpG can be interpreted by focusing on 2 considerations: the first is that once the discharge process starts, at the extreme left and right sides of the port, flow passages are narrow and the pressure difference is very high. In such a situation, the air rushes within the low pressure chamber forming jets at a very high speed within small areas. As one of these jets reaches the control volume it creates a peak like profile as the ones observed on figure 10. Secondly, as the rotors rotate further the ports will be open more causing the air jet stream to move towards the centre of the V-section and reduces its velocity. This explains why the velocity peaks in figures 10(c) and (d) move up and to the right.

## **CONCLUSIONS**

Axial mean flow measurements and the corresponding turbulent fluctuation were measured inside a screw compressor both upstream and downstream the discharge port with high spatial and temporal resolution using laser Doppler velocimetry (LDV) at a rotational speed of 1000 rpm and a pressure ratio of 1.0. The most important findings can be summarised as:

1 The results of the axial mean and RMS velocities were successfully captured using gated post processing method with angular resolutions of up to  $1.5^\circ$  in the rotor chambers and  $1.0^\circ$  in the discharge chamber. A high data rate pressure transducer was employed within the working chamber to provide an additional set of data to characterise not only the axial velocity field but also the instantaneous pressure.

2 The axial velocity distribution within the discharge chamber is strongly correlated with angular rotor position. For example, within the high pressure gradient position (HpG) zone, the velocity is influenced mainly by the pressure difference between the chambers at the opening of the discharge port. On the other positions, where strong gradient are not present, the velocity is mainly influenced by the rotor motion.

3 Within the HpG region jet like flow into the discharge chamber was found. These jets create peaks in the mean velocities and high turbulence flow.

Overall, these data will be used to establish a reliable CFD model of the flow and pressure distribution within twin screw machines, both as input data and also to verify the predicted results, which can then be used as a tool to further improve the design of screw compressors and expanders.

## **ACKNOWLEDGEMENT**

Financial support from EPSRC (Grant EP/C541457/1), Trane, Lotus and Gardner Denver is gratefully acknowledged. The authors would like to thank Michael Smith, Jim Ford and Grant Clow for valuable technical support during the course of this work.

## REFERENCES

1. **Guerrato D, Nouri J.M, Stosic N. and Arcoumanis, C. 2007** Axial flow and pressure characteristics within a double screw compressor. *3<sup>rd</sup> Int. Conf. Optical and Laser Diagnostics, ICOLD*, 23-25 May 2007, London.
2. **Stosic N, 1998**, On gearing of helical screw compressor rotors, *Proc IMechE*, **213(C)**, pp. 587-594.
3. **Nouri J.M, Guerrato D., Stosic N. and Kovacevic A, 2007**, Cycle-resolved velocity measurements within a screw compressor. *18<sup>th</sup> Int. Compressor Eng. Conf.*, 17-20 July 2007, Purdue.
4. **Nouri, J.M, Guerrato, D, Stosic N. and Arcoumanis C, 2007**, Axial Flow Characteristics within a Screw Compressor. *Accepted by ASHRAE Research Journal*.
5. **Kovacevic A, Stosic N. and Smith I.K, 2002**, CFD Analysis of Screw Compressor Performance. *In: Advances of CFD in Fluid Machinery Design*, edited by Elder R.L., A. Tourlidakis and M.K. Yates, Professional Engineering Publishing, London.
6. **Kampanis N, Arcoumanis C, Kato R, Kometani S, 2001**, Flow, combustion and emissions in a five-valve research gasoline engine. *SAE Paper 2001-013557*.
7. **Yan Y, Gashi S, Nouri J.M, Lockett R.D. and Arcoumanis C, 2005**, Investigation of spray characteristics in a spray guided DISI engine using PLIF and LDV, *2<sup>nd</sup> Int. Conference on Optical Diagnostics, ICOLD*, London, September 2005.
8. **Liu C.H, Nouri J.M, Vafidis C. and Whitelaw J.H, 1990**, Experimental study of flow in a centrifugal pump, *5<sup>th</sup> International Symposium on Applications of Laser Techniques to Fluid Mechanics*, Lisbon, July 1990.
9. **Arcoumanis C, Martinez-Botas R, Nouri J.M. and Su C.C, 1997**, Performance and exit flow characteristics of mixed flow turbines. *International Journal of Rotating Machinery*, **3**, No. 4, pp. 277-293.
10. **Arcoumanis C, Martinez-Botas R, Nouri J.M. and Su C.C, 1998**, Inlet and exit flow characteristics of mixed flow turbines. *ASME, Int. gas Turbine and Aeroengine Congress and Exhibition*, Paper 98-GT-495, Stockholm, June 1998.
11. **Zaidi S.H. and Elder, R.L, 1993**, Investigation of flow in a radial turbine using laser anemometry. *ASME, Int. Gas Turbine and Aeroengine Congress and Exhibition, Cincinnati*, paper 93-GT-55, Ohio, May 1993.
12. **Hockey R.M. and Nouri J.M, 1997**, Turbulent flow in a baffled vessel stirred by a 70 pitched blade impeller. *Chem. Eng. Science*, **51**, pp. 4405-4421.